6-26-2011

Establishing Confidence in Surface Wave Determined Soil Profiles

Paul Michaels
Boise State University

 DOI: 10.1061/41183(418)88

Establishing Confidence in Surface Wave Determined Soil Profiles

P. Michaels[1], Member ASCE

[1]Center for Geophysical Investigation of the Shallow Subsurface, Boise State University, 1910 University Drive, Boise, Idaho 83725-1535 , PH (208) 426-1929; FAX (208) 426-1631; email: pm@cgiss.boisestate.edu

ABSTRACT

Surface waves can be used to determine the shear velocity profile from the ground surface to some depth limited by the spectral band of the seismic source. A number of factors influence the uncertainties of the determined profile. The field acquisition factors include the deployment geometry of geophones, the spectral characteristics of the geophones, recording instruments, and seismic source. A key data processing factor is the determination of a dispersion curve from the field recordings. Finally, there are important choices in conducting the inversion of the dispersion curve which leads to the final soil profile. Even if the field factors and acquired data are fixed, determination of the dispersion and the inversion decisions will have a strong influence on the final result. Different engineers will make different decisions, and a range of soil profiles can be expected. Assessment of this variability was the goal of the Surface Wave Benchmark Study sponsored by the Geophysical Engineering Committee of ASCE. Participants were invited to analyze as little or as much of the data as they wished. This paper documents one participant's analysis of a selected set of the data taken at a single location. A key finding documents how a lack of low frequency content limits the maximum depth for which one can have confidence in the soil profile.

INTRODUCTION

The near surface shear-wave velocity profile is of interest in a number of applications. These include earthquake soil dynamics, the response of foundations and structures to both earthquakes and vibrations due to construction, pile driving, and blasting. The method has also been applied to the evaluation of pavements. Frequently employed non-invasive surface wave methods used to determine the shear-wave soil profile include Spectral Analysis of Surface Waves (SASW) and Multichannel Analysis of Surface Waves (MASW) (Penumadu & Park, 2005). There has been interest in evaluating these non-invasive techniques (Tran & Hiltunen, 2008). Additionally, the uncertainty in the analysis and the impact on application risks has begun to be considered (Hiltunen *et al.* , 2006; Marosi & Hiltunen, 2004). Typical practice involves the acquisition of Rayleigh wave data using a surface seismic source and geophone receiver deployment. Recordings are digitally processed to yield phase velocity dispersion, and the dispersion curves are inverted to a 1-D shear-velocity profile (Yuan &

Nazarian, 1993). The depths penetrated depend on the recorded signal spectrum. Recent advances include an effort to extend the low frequency content of data to increase the maximum depth for which reliable results can be obtained (Rosenblad *et al.* , 2008; Rosenblad & Li, 2009).

In an attempt to further understand the variable factors leading to risk assessment and uncertainty with surface wave methods, the Geophysical Engineering Committee (GEC) of the ASCE Geo-Institute sponsored a benchmark study. Practitioners were invited analyze sets of surface wave data collected at the National Geotechnical Experimentation Site (NGES) at Texas A&M University (TAMU). This paper is one of those investigations into the risk assessment of surface wave analysis.

SELECTED DATA

This paper focuses on one of the data sets, test site 98-220. These data were collected for Multi-channel Analysis of Surface Waves (MASW). The active source was a sledge hammer located at station 78, 6.10 meters (20 ft) from the nearest geophone. Geophones were placed 0.6096 meters (2 ft) apart extending away from the source to a maximum offset of 43.28 meters (142 ft). The 62 geophones had a natural frequency of 4.5 Hz and were oriented vertically. The data were digitized at a .00078125 second sample interval, anti-alias filter of 500 Hz. The pre-trigger delay was about 10% of the 12.8 second record length. A selected portion of the data are shown in Figure 1. Figure 2 shows an all-pole estimate of the available signal spectrum.

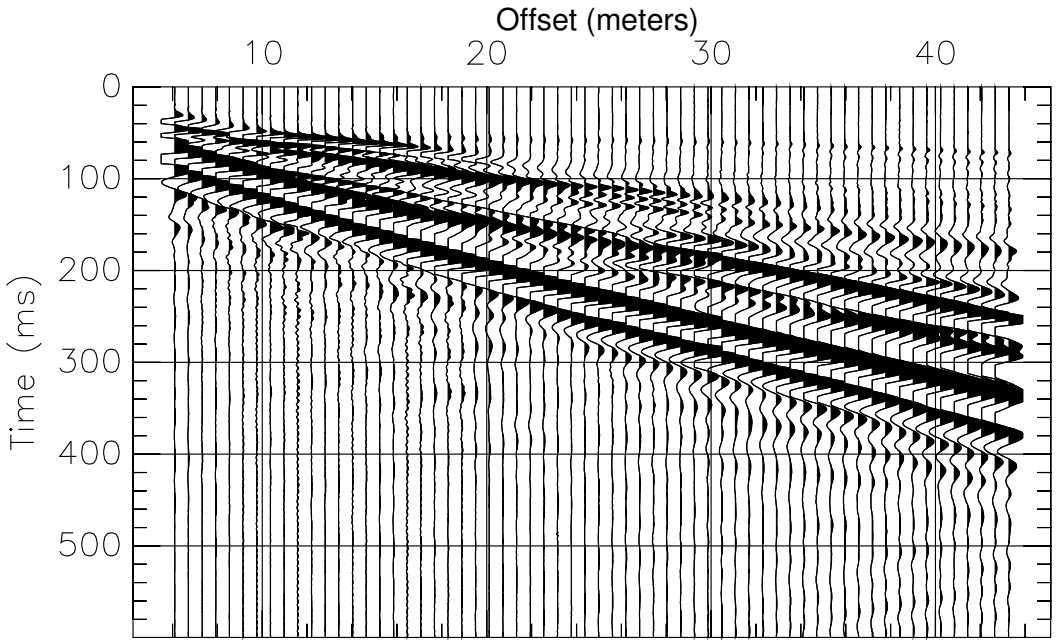

Figure 1. Selected portion of data. Each geophone channel has been rescaled by its norm to remove amplitude decay with offset and improve visibility of the waveforms.

To determine the available signal spectrum, a Yule-Walker all pole spectrum (Karl, 1989) was computed from the average of the auto-correlations (all 62 channels).

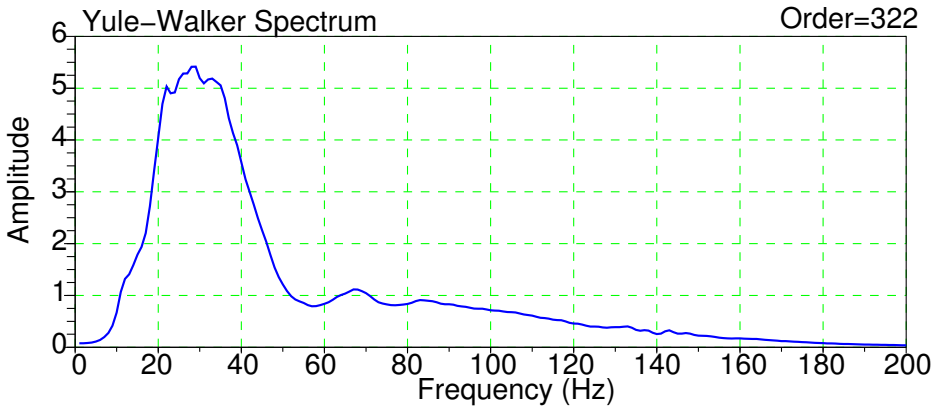

Figure 2. All pole Yule-Walker spectrum from averaged autocorrelations of the test data. Small DC shifts were removed if present prior to computation of the spectrum. The signal band from 5 Hz to 47 Hz was chosen for analysis.

Initial signal analysis showed that the fundamental mode dominated the dispersion at frequencies below about 50 Hz. The signal band from 5 to 47 Hz was chosen for analysis. This choice was limited by the decision to analyze only the fundamental mode, and use as low a frequency as could be justified by the spectral estimate. The lowest available frequency sets the maximum effective depth of exploration.

DISPERSION AND MASW ANALYSIS

The dispersion was computed in the time domain by beam steering data filtered at 1 Hz intervals (Michaels, 1998). Error bars were computed from the measured signal shifts about the best fit velocity trend and are shown for 95% confidence in Figure 3-(a) (assumes normal distribution). The measured phase velocity dispersion is plotted as distinct symbols with error bars that often fall within the plot symbol except at the low frequencies where signal strength is vanishing. The solution model is shown in Figure 3-(b). The parameterization of the soil profile is described in the next section. There are 5 control points. The depth of exploration varies with frequency as can be seen in Figure 3-(c). Only the lowest frequencies probe to a depth of 30 meters, and those results are the most uncertain due to the lack of low-frequency signal strength.

Parameterization of Soil Profile Many investigators parameterize the soil profile as a number of layers, each layer having a shear velocity as an unknown parameter. In such a choice, it has been shown that the uncertainty in shear wave velocity increases with the number of layers (Hiltunen *et al.* , 2006). That is not the case with the parameterization here. Parameters are control point pairs of depth and shear velocity. Linear interpolation of elastic moduli is performed in constant layer steps. In Figure 3, the step size is 0.2 meters. The mass density, ρ, of the soil has been held constant. At each control point, shear modulus is determined by

$$G = {V_s}^2 \cdot \rho \quad ,$$

where G is shear modulus and V_s is the control shear velocity. Poisson's ratio, $\sigma = 1/3$, is also held constant to determine P-wave velocity and Lame's constant, λ. Thus,

$$V_p = V_s \cdot \sqrt{\frac{2(1-\sigma)}{(1-2\sigma)}} \quad ,$$

and

$$\lambda = \left({V_p}^2 - 2{V_s}^2\right)\rho \quad .$$

Linear interpolation between control points of G, λ, and ρ assigns values of V_s, V_p, and ρ for each layer step. Thus, the number of parameters is greatly reduced to about twice the number of control points. Fixing parameters at the top and bottom reduces the number of unknowns further.

The inversion algorithm iteratively solves for depth and shear velocity of each control point so as to minimize the difference between the observed and computed dispersion curve. The inversion method chosen was truncated singular value decomposition (Menke, 1989). Only the 5 largest singular values were employed in this paper. The surface control point was fixed at zero depth, velocity free to vary. The bottom depth control point was fixed at 16 meters, but velocity was free to vary at that point. Properties remain constant below the bottom control point.

The results of the inversion shown in Figure 3 are tabulated in Table 1. The confidence limits determined in measuring the dispersion curve were used to compute the confidence limits of the solution parameters (non-fixed control depths and shear velocity, V_s, at all depth points). The mapping of uncertainties from measured to computed quantities is done by the formula (Menke, 1989)

$$C_m = H \cdot C_d \cdot H^T \quad ,$$

where C_m is the covariance matrix for solved parameters, H is the generalized inverse, and C_d is the covariance matrix of the data. Variance estimates were then scaled for 95% confidence assuming normally distributed errors. The covariance matrix for the dispersion measurements, C_d, was diagonal with the variance for each measured phase velocity on the diagonal. These diagonal elements correspond to the error bars of Figure 3-(a).

Table 1. Inversion Results with 95% Confidence Limits. Note that there are two degrees of freedom (depth, velocity) of uncertainty for each control point in the solution.

Depth (m)	V_s (m/s)	V_p (m/s)	ρ (kg/m^3)
0 $\pm$0.000	128.344 $\pm$0.656	256.689	2169.
1.664 $\pm$0.189	153.404 $\pm$0.085	306.808	2169.
3.184 $\pm$0.980	217.274 $\pm$0.326	434.548	2169.
6.596 $\pm$1.350	165.638 $\pm$0.326	331.276	2169.
16.000 $\pm$0.000	387.437 $\pm$1.969	774.873	2169.

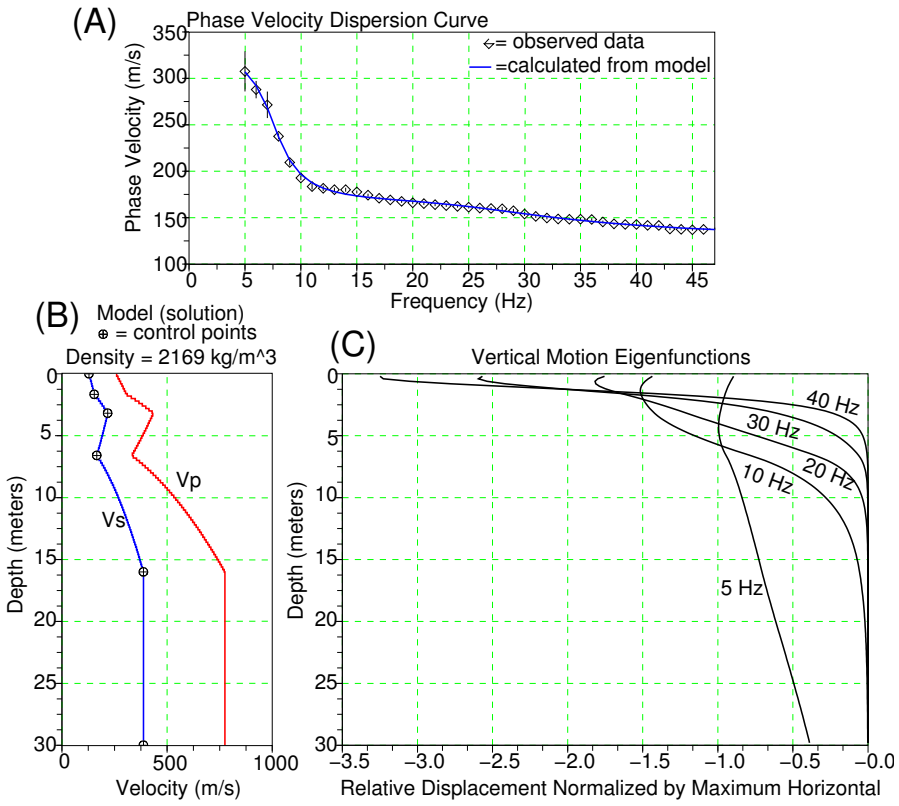

Figure 3. (A) Dispersion curve showing observed data and calculated curve from the solution. (B) The solution shear wave velocity showing the 5 control points. Linear interpolation of elastic moduli between control step wise by 0.2 meter layers. Poisson's ratio set at $\sigma = 1/3$, density held constant at $\rho = 2169 kg/m^3$. (C) Vertical-motion eigenfunctions for frequencies shown, normalized by horizontal motion at each frequency. High frequencies sense shallow soil, low frequencies probe deeper. The majority of the motion is above 16 meters depth.

ALTERNATIVE FAST AND SLOW SOLUTIONS

To better estimate the risk of soil characterization by surface waves, the 95% confidence limits of Table 1 were applied to determine a maximally fast and slow alternative to the best solution. The fast alternative was formed by shifting the control depths toward the surface by the 95% error limits, and increasing the shear-wave velocity by the corresponding error limits. The slow alternative was formed by increasing the depth control points and decreasing the shear-wave velocities. The results are shown in Figure 4. Note that there are two degrees of freedom (velocity and depth) for each error estimate.

RISK ANALYSIS

The context for this paper is the problem of estimating the shear-wave velocity profile in the first 30 meters. Research on characteristics important to earthquake engineering have resulted in changes to building codes (Dobry *et al.* , 2000). Current

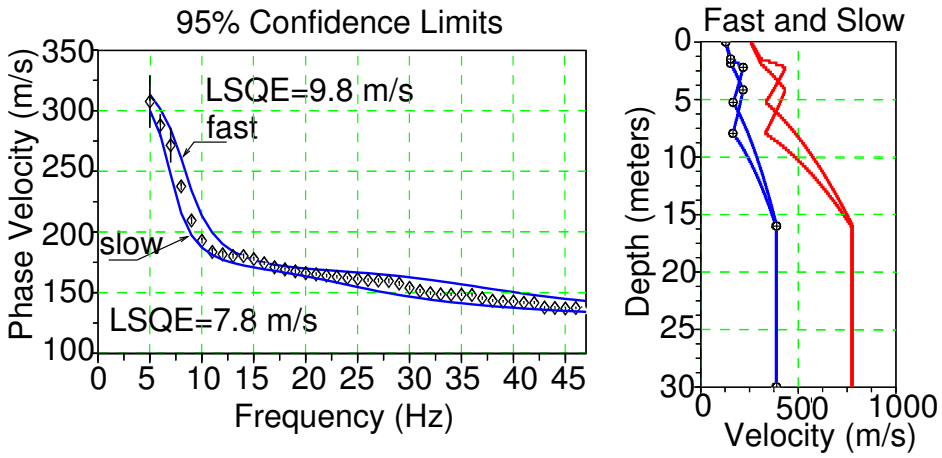

Figure 4. The computed dispersion from the two alternative fast and slow limiting cases. Since there are two degrees of freedom (depth and velocity) at each control point, the Table 1 uncertainties are larger than might be perceived by a casual observer.

building codes refer to this as Vs_{30}. It is computed for a layered profile by formula 36-1 of UBC-97, for example.

$$Vs_{30} = \frac{\sum Z_i}{\sum (Z_i / Vs_i)}$$

Uncertainties in measured dispersion do not affect Vs_{30} enough to change the soil profile type which is *SD*, *stiff soil*. The definition of *stiff soil* is $[180 < Vs_{30} < 360]\, m/s$. Table 2 summarizes the results of the computation for the solution and the two limiting cases.

Table 2. Shear velocity, Vs_{30}, from alternative soil profiles.

Case	Vs_{30}
slow	270 m/s
solution	277 m/s
fast	286 m/s

SITE AMPLIFICATION

To evaluate the possible risks associated with Vs_{30} in the context of site amplification, we can consider the amplification which would result from bedrock shear velocities that might underlie the soil profile. Figure 5 shows two cases for bedrock, $Vs_{br} = 387.5m/s$ and $Vs_{br} = 1000m/s$. The slower case corresponds to the fastest velocity determined from the surface wave data.

As can be seen from Figure 5, the faster bedrock assumption produces over twice as much amplification. This then begs the following question. Could the surface wave data sense such a faster bedrock at 30 meters depth, were it to be present? To evaluate this question, we can recompute the dispersion with the faster bedrock below the

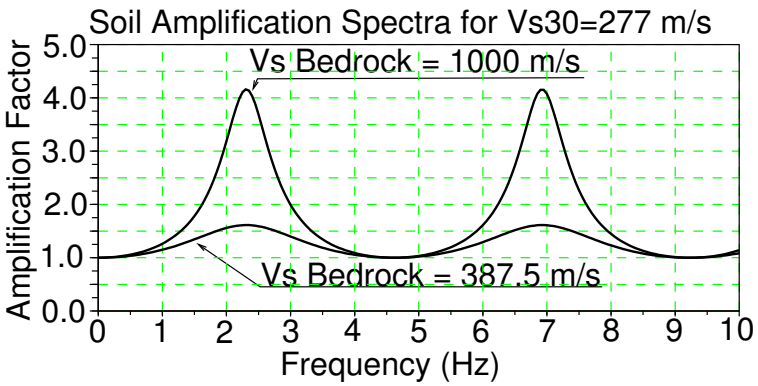

Figure 5. The site amplification factors for two possible bedrock velocities below a 30 meter soil equivalent to the Vs_{30} determined from the surface wave data. No damping other than radiation damping is assumed.

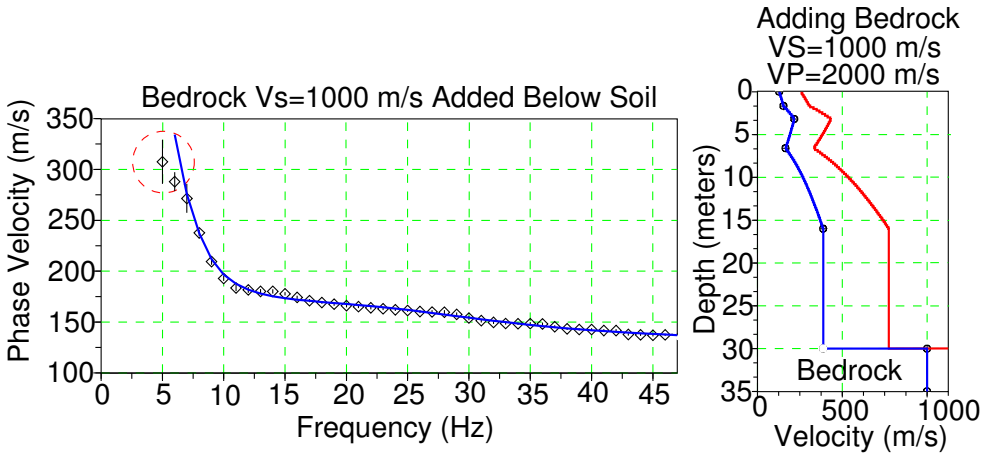

Figure 6. The addition of the faster bedrock only changes the computed dispersion at frequencies below 7 Hz (see dashed circle). This illustrates the value of low frequencies in sensing the soil profile at a depth of 30 meters.

soil model of Figure 3. The result is shown in Figure 6. Without the two measurements at 5 and 6 Hz, the surface wave data would not be able to detect the faster bedrock at a 30 meter depth, were it present.

CONCLUSIONS

The shear-velocity soil profile may be parameterized in different ways. Here, this was done by step wise linear interpolation of the elastic moduli between sparse control points. Confidence limits were computed for both depth and velocity. The sledge hammer source just barely investigates depths down to 30 meters as is evident from the motion-stress eigenfunctions (see Figure 3-(c)) and the circled points in Figure 6. Low frequencies (below 7 Hz) are needed to reduce the risk in estimating soil amplification.

ACKNOWLEDGMENTS

The author expresses his thanks to the Geophysical Engineering Committee of the ASCE GeoInstitute for conducting this benchmark testing, and to National Science Foundation and Texas A&M University for their respective roles in supporting the data acquisition.

REFERENCES

Dobry, R., Borcherdt, R. D., Crouse, C. B., Idriss, I. M., Joyner, W. B., Martin, G. R., Power, M. S., Rinne, E. E., & Seed, R. B. (2000). New Site Coefficients and Site Classification System Used in Recent Building Seismic Code Provisions. *Earthquake Spectra*, 16(1), 41–67.

Hiltunen, Dennis R., Marosi, Karen T., & Gardner, Jason M. (2006). Methodologies to Assess SASW Shear Wave Velocity Uncertainty. *Pages 94–94 of:* DeGroot, Don J., DeJong, Jason T., Frost, J. David, & Baise, Laurie G. (eds), *GeoCongress 2006: Geotechnical Engineering in the Information Technology Age*, vol. 187. ASCE.

Karl, J. H. (1989). *An Introduction to Digital Signal Processing*. Academic Press.

Marosi, Karen T., & Hiltunen, Dennis R. (2004). Characterization of Spectral Analysis of Surface Waves Shear Wave Velocity Measurement Uncertainty. *Journal of Geotechnical and Geoenvironmental Engineering*, 130(10), 1034–1041.

Menke, W. (1989). *Geophysical data analysis, discrete inverse theory*. Academic Press. San Diego 289pgs.

Michaels, P. (1998). In situ determination of soil stiffness and damping. *Journal of Geotechnical and Geoenvironmental Engineering*, 124(8), 709–719.

Penumadu, Dayakar, & Park, Choon B. (2005). Multichannel Analysis of Surface Wave (MASW) Method for Geotechnical Site Characterization. vol. 158. ASCE.

Rosenblad, Brent L., & Li, Jianhua. (2009). Performance of Active and Passive Methods for Measuring Low-Frequency Surface Wave Dispersion Curves. *Journal of Geotechnical and Geoenvironmental Engineering*, 135(10), 1419–1428.

Rosenblad, Brent L., Stokoe, Kenneth H., II, Li, Jianhua, Wilder, Brad, & Menq, Farn-Yuh. (2008). Deep Shear Wave Velocity Profiling of Poorly Characterized Soils Using the NEES Low-Frequency Vibrator. vol. 318. ASCE.

Tran, Khiem T., & Hiltunen, Dennis R. (2008). A Comparison of Shear Wave Velocity Profiles from SASW, MASW, and ReMi Techniques. vol. 318. ASCE.

Yuan, Deren, & Nazarian, Soheil. (1993). Automated Surface Wave Method: Inversion Technique. *Journal of Geotechnical Engineering*, 119(7), 1112–1126.